

Enhanced violation of a Leggett-Garg inequality under nonequilibrium thermal conditions

Juan C. Castillo,¹ Ferney J. Rodríguez,¹ and Luis Quiroga¹

¹*Departamento de Física, Universidad de los Andes, A.A. 4976 Bogotá, D.C., Colombia*

(Dated: January 27, 2023)

We investigate both analytically and numerically violations of a Leggett-Garg inequality (LGI) for a composite quantum system in contact with two separate reservoirs at different temperatures. Remarkably we find that LGI violations can be enhanced when a heat current is established at low temperatures in a steady-state regime. Based on a Kraus operator decomposition of the non-unitary evolution for a system formed by two interacting spins or quantum bits, we provide analytical support for power law relations between dissipation strength and mean temperature in the borderlines separating parameter regions where non-equilibrium conditions affect differently the maximal LGI violation. Furthermore, a correspondence between spatial and temporal correlation inequalities is shown to persist even in such nonequilibrium thermal settings.

PACS numbers: 03.67.Mn, 03.65.Ud, 65.40.Gr

Since the seminal work by John Bell [1] about quantum spatial correlations, an ever increasing number of experiments has been devoted to test the foundations of quantum mechanics. In a parallel way, and triggered by those tests, practical schemes for conveying quantum information have flourished. New aspects of the fascinating world of quantum correlations arose when temporal, instead of spatial, correlations were proposed by Leggett and Garg [2], and subsequently by many other authors [3–5]. In those works different inequalities between two-time correlations have been proposed that should hold whenever a classical description is valid. An emerging Leggett-Garg inequality (LGI) violation would mark a borderline between the classical and quantum worlds. Of special interest has been the guide provided by LGI for testing macroscopic realism in condensed matter systems [6–12] as well as in quantum optics setups [13, 14] where focus has been put on LGI violations for open quantum systems in contact with realistic reservoirs.

On the other hand, one of the most important challenges to detect superposition of quantum macroscopic states is the fragility of these states caused by decoherence effects. Despite the ubiquitous presence of non-equilibrium situations in quantum mesoscopic and macroscopic physics, few formal results about quantum correlations in such regimes are available [15–18]. Many efforts encompassing a large variety of physical systems have been directed to study the effects of spatial correlations, as measured by the concurrence [15, 19, 20] and quantum discord (QD) [21], under non-equilibrium gradients. However, LGI studies have been very scarce in systems out of thermodynamic equilibrium, although time correlations in condensed matter systems show complex and interesting behaviors, like those observed in ultracold atom systems [22], inductively (capacitively) coupled flux (charge) superconducting qubits [23], and even energy transfer processes in photosynthetic purple bacteria [24].

How do thermal non-equilibrium conditions affect quantum two-time correlations? From a theoretical point of view important insights have been given in Ref.[25] where nanothermodynamics relevance of quantum coherences has been addressed. From the experimental side Ref.[26] shows an ele-

gant experiment where thermal and electric currents interfere in a Josephson junction. Here, we propose a set up where the relationship between two-time quantum correlations and out-of-equilibrium thermal conditions can be systematically explored through the LGI violations. Here, we examine a LGI for a two-qubit system and show that violations are enhanced when a heat current, \mathcal{J} , is flowing through it.

For nonequilibrium dynamics, what is the optimal relationship between dissipation strength (Γ) and temperature range (T) which allows the detection of quantum correlations through macroscopic transport measurements? The theoretical approach we provide, in terms of Kraus operator dynamics evolution, gives a general framework to identify non-classical features through LGI violations for quantum systems in contact with two memoryless (Markovian) separate reservoirs at different temperatures. We find that dissipation, inter-qubit interactions and mean temperature compete, resulting in a rich T - Γ phase diagram where power-law relations mark the boundaries between different zones where LGI violations are either absent, decreasing or increasing with an applied temperature gradient.

The two-time correlation inequality, LGI, extends the well-known Bell inequality (designed to probe spatial quantum correlations) to the time domain. One form the LGI can take is [2–4, 27]:

$$F(t_1, t_2, t_3) = C(t_1, t_2) + C(t_2, t_3) - C(t_1, t_3) \leq 1 \quad (1)$$

where $C(t_i, t_j)$ is the two-time correlation of a dichotomic observable \hat{Q} (eigenvalues $a=\pm 1$) between times t_i and t_j and $t_1 < t_2 < t_3$. To evaluate $F(t_1, t_2, t_3)$ in Eq.(1), a Kraus operator $\hat{K}(t)$ approach has been used [28, 29]. In the following we limit ourselves to a steady-state regime. Due to this last assumption, two-time correlations depend only on the time difference between two instants, which implies the non-invasive measurement requirement in LGI settings [4]. The steady-state or long time limit of the density operator will be denoted as $\hat{\rho}_{ss} = \hat{\rho}(t \rightarrow \infty)$. By choosing in $F(t_1, t_2, t_3)$ all three times t_1, t_2 and t_3 in the steady-state regime and fixing them as $t_1 = 0, t_2 = \tau$ and $t_3 = 2\tau$, the two-time correlation function can finally be expressed as (see Ref. [29])

$C(\tau) = 1 - 4p^+ + 4\text{Re}[g(\tau)]$, allowing us to rewrite Eq.(1) as

$$F(0, \tau, 2\tau) = 1 - 4p^+ + 4\text{Re}[2g(\tau) - g(2\tau)] \leq 1 \quad (2)$$

where $p^+ = \text{Tr}\{\hat{\Pi}^+ \hat{\rho}_{ss}\}$ denotes the long time limit of the probability for obtaining the result $a = +1$, $\hat{\Pi}^+$ the corresponding projector and

$$g(\tau) = \text{Tr}\left\{\hat{\Pi}^+ \sum_{\nu} \hat{K}_{\nu}(\tau) \hat{\Pi}^+ \hat{\rho}_{ss} \hat{K}_{\nu}^{\dagger}(\tau)\right\} \quad (3)$$

This last term is of highest importance for the present work as it is the responsible for LGI violations.

We consider a bipartite quantum system in contact with separate thermal baths at different temperatures T_1 and T_2 . To be specific, the quantum system of interest is a two spin chain described by:

$$\hat{H}_Q = \frac{\epsilon_1}{2} \hat{\sigma}_{z,1} + \frac{\epsilon_2}{2} \hat{\sigma}_{z,2} + V(\hat{\sigma}_1^+ \hat{\sigma}_2^- + \hat{\sigma}_1^- \hat{\sigma}_2^+) \quad (4)$$

where ϵ_i is the energy splitting of the i -th qubit, $\hat{\sigma}_{z,i}^{\pm}$ denote Pauli matrices and V describes the inter-qubit interaction strength. The baths are represented by sets of harmonic oscillators with Hamiltonians $\hat{R}_i = \sum_n \Omega_{n,i} \hat{a}_{n,i}^{\dagger} \hat{a}_{n,i}$ where $\hat{a}_{n,i}^{\dagger}$ ($\hat{a}_{n,i}$) creates (destroys) an excitation in the i -th reservoir while the coupling of each qubit with its separate reservoir is given by $\hat{H}_{int,i} = \hat{\sigma}_i^+ \sum_n g_n^{(i)} \hat{a}_{n,i} + \hat{\sigma}_i^- \sum_n g_n^{(i)} \hat{a}_{n,i}^{\dagger}$ where $g_n^{(i)}$ denote the system-bath coupling strengths. In the Born-Markov framework the system-bath couplings are essentially determined by the bath spectral density of the form $J_i(\omega) = \Gamma n_i(\omega)$ where Γ denotes the coupling strength (taken identical for both reservoirs) and $n_i(\omega) = (e^{\beta_i \omega} - 1)^{-1}$, the Bose-Einstein distribution of excitations in the i -th bath at inverse temperature β_i [15]. For the sake of simplicity we limit ourselves to the *symmetric-qubit* case, i.e. $\epsilon_1 = \epsilon_2 = \epsilon$. In the following, energy, frequency and temperature will be measured in units of the inter-qubit interaction strength V while time will be expressed in units of V^{-1} by letting $\hbar = K_B = 1$. We thus set $\tilde{\epsilon} = \epsilon/V$, $\tilde{\Gamma} = \Gamma/V$, $\tilde{\omega} = \omega/V$, $\tilde{T} = T/V$, and $\tilde{\tau} = V\tau$.

The eigenstates for the qubit Hamiltonian in Eq.(4) are given, in the $\hat{\sigma}_{z,i}$ basis, by: $|1\rangle = |+, +\rangle$, $|2\rangle = (|+, -\rangle - |-, +\rangle)/\sqrt{2}$, $|3\rangle = (|+, -\rangle + |-, +\rangle)/\sqrt{2}$ and $|4\rangle = |-, -\rangle$. The non-equilibrium thermal steady-state density operator for the pair of qubits turns out to be diagonal in this basis taking the form of a direct product as [15]

$$\hat{\rho}_{ss} = \hat{\rho}_1^{ss} \otimes \hat{\rho}_2^{ss} = \sum_{\alpha=1}^4 c_{\alpha} |\alpha\rangle \langle \alpha| \quad (5)$$

where $\hat{\rho}_j^{ss}$ denotes the steady-state density operator of a *single fictitious* qubit of energy splitting $\tilde{\omega}_j$ in thermal equilibrium with a single reservoir at an effective temperature corresponding to the mean number of thermal excitations as given

by $n(\tilde{\omega}) = \frac{1}{2} \sum_{i=1,2} n_i(\tilde{\omega})$ with index i representing each separate thermal bath. The two effective qubits have energy splittings given by $\tilde{\omega}_1 = |\tilde{\epsilon} - 1|$ and $\tilde{\omega}_2 = \tilde{\epsilon} + 1$. Thus, $\hat{\rho}_j^{ss} = \text{diag}\left\{\frac{n(\tilde{\omega}_j)}{2n(\tilde{\omega}_j)+1}, \frac{n(\tilde{\omega}_j)+1}{2n(\tilde{\omega}_j)+1}\right\}$ implying that the steady-state spin chain density operator in Eq.(5) does not depend on the system-bath coupling strength Γ . Of special interest for the discussion of results below are the coefficients c_2 and c_3 in Eq.(5), given by $c_2 = \left(\frac{n(\tilde{\omega}_1)}{2n(\tilde{\omega}_1)+1}\right) \left(\frac{n(\tilde{\omega}_2)+1}{2n(\tilde{\omega}_2)+1}\right)$ and $c_3 = \left(\frac{n(\tilde{\omega}_1)+1}{2n(\tilde{\omega}_1)+1}\right) \left(\frac{n(\tilde{\omega}_2)}{2n(\tilde{\omega}_2)+1}\right)$, which determine the heat current across the quantum system by the annihilation of an excitation from one reservoir and the subsequent creation of another excitation in the other reservoir through a flip-flop process in the two-spin chain. Notice that in the special case $\tilde{\epsilon} = 1$, one of the fictitious qubits has zero splitting, $\tilde{\omega}_1 = 0$, which is equivalent to having at least one bath at infinite temperature since $n(\tilde{\omega}) \rightarrow \infty$. In order to assess under which conditions the LGI can be violated, $F(0, \tilde{\tau}, 2\tilde{\tau}) > 1$ in Eq.(2), we pick the *single* qubit operator $\hat{Q} = \hat{\sigma}_{z,1}$ as the dichotomic observable to evaluate the LGI. The projector to the $|+\rangle$ eigenspace for this observable is $\hat{\Pi}^+ = |+\rangle \langle +| \otimes \hat{\mathbb{I}} = |1\rangle \langle 1| + \frac{1}{\sqrt{2}} \sum_{\alpha=2}^3 |\alpha\rangle \langle \alpha|$.

To gain physical insight on quantum two-time correlations and LGI violations for a nonequilibrium thermal spin chain, we first consider a simple case: once the spin chain reaches the nonequilibrium steady-state regime, we proceed to break its couplings to the heat reservoirs and let it evolve unitarily under the action of Hamiltonian \hat{H}_Q . In this case, the LGI- F function can be analytically evaluated, yielding to

$$F(0, \tilde{\tau}, 2\tilde{\tau}) = 1 + r_{23} [2 \cos(2\tilde{\tau}) - \cos(4\tilde{\tau}) - 1] \quad (6)$$

which only involves, through $r_{23} = c_2 + c_3$, the density matrix elements corresponding to eigenstates $|2\rangle$ and $|3\rangle$, as expected. Under the sole action of \hat{H}_Q the states $|1\rangle$ and $|4\rangle$ are thus decoupled from the other two states. It is then easily seen that $F(0, \tilde{\tau}, 2\tilde{\tau})$ begins at a value of 1 for $\tilde{\tau} = 0$. The LGI is violated during an initial time interval from $\tilde{\tau} = 0$ to $\tilde{\tau} = \pi/4$, reaching a maximal violation when $\tilde{\tau} = \pi/6$ irrespective of the bath temperatures. However, the maximum value of the LGI violation (MLGI), as defined by $MLGI = F^{(Max)}(0, \tilde{\tau}, 2\tilde{\tau}) - 1 \geq 0$, does depend on r_{23} and consequently on the bath temperatures.

Now, we restore the couplings of the spin chain with the baths which makes it imperative to evaluate the quantum open system's Kraus operators numerically (details will be presented elsewhere). Using this procedure, the two-time correlation function $C_N(\tilde{\tau})$ can be safely approximated by a fitting correlation function of the form $C_F(\tilde{\tau}) = 1 - r_{23} \left[1 - e^{-\tilde{\Gamma}_V \tilde{\tau}} \cos(2\tilde{\tau})\right]$, where $\frac{\tilde{\Gamma}_V}{\tilde{\Gamma}} = \sum_{j=1}^2 [2n(\tilde{\omega}_j) + 1]$.

The fit is good enough that $|C_N(\tilde{\tau}) - C_F(\tilde{\tau})| \leq 10^{-5}$ for the full numerical results in the range $\tilde{\tau} < 6$, validating our analytical results described below. Thus, by using the fitting correlation functions, $C_F(\tilde{\tau})$, the LGI in Eq.(2) can be written

as

$$F(0, \tilde{\tau}, 2\tilde{\tau}) = 1 + r_{23} \quad (7)$$

$$\left[2e^{-\tilde{\Gamma}_V \tilde{\tau}} \cos(2\tilde{\tau}) - e^{-2\tilde{\Gamma}_V \tilde{\tau}} \cos(4\tilde{\tau}) - 1 \right] \leq 1$$

In contrast to the steady-state nonequilibrium thermal concurrence [15, 19] and QD [21], the LGI- $F(0, \tilde{\tau}, 2\tilde{\tau})$ depends explicitly on the dissipation rate $\tilde{\Gamma}$. It is of special interest to relate the LGI- F function with a measurable transport quantity such as the heat current flowing through the spin chain in response to a temperature gradient. An analytical expression for the heat current under a temperature gradient, $\Delta\tilde{T} = \tilde{T}_1 - \tilde{T}_2$, as calculated from $\mathcal{J}(\Delta\tilde{T}) = \text{Tr} \left\{ \hat{H}_Q \hat{\mathcal{L}}_1 \right\}$ can be found in Ref.[15]. Although a closed equation relating $F(0, \tilde{\tau}, 2\tilde{\tau})$ with the heat flow is possible, the expression is cumbersome and will be skipped here, since their relationship is still better appreciated by looking at the figures as discussed below.

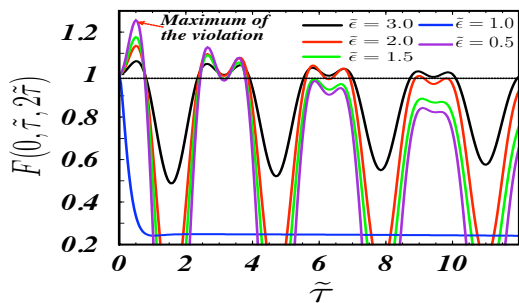


FIG. 1: (Color online). LGI- F function at thermal equilibrium, i.e. $\Delta\tilde{T} = 0$. $F(0, \tilde{\tau}, 2\tilde{\tau})$ for symmetrical qubits with different splittings and identical bath temperatures $\tilde{T}_1 = \tilde{T}_2 = 1.1$. The LGI is violated whenever $F(0, \tilde{\tau}, 2\tilde{\tau}) > 1$.

To illustrate the behavior of the MLGI violation under nonequilibrium thermal conditions we proceed to consider realistic parameters. The set of chosen parameters (in V units), for the results we discuss below, are in the actual experimental range for superconductor qubits $\tilde{\epsilon}_i \sim 5$ and $\tilde{\Gamma} \sim 10^{-3}$ [23] while for excitons in biological photosynthetic systems $\tilde{\epsilon}_i \sim 1.4$ and $\tilde{\Gamma} \sim 0.4$ [24]. First, we analyze results for the equilibrium case, i.e. $\Delta\tilde{T} = 0$. As plotted in Fig. 1, violations of LGI are still visible up to $\tilde{\tau} = 10$ for an equilibrium temperature $\tilde{T}_M = \tilde{T}_1 = \tilde{T}_2 = 1.1$. For weak inter-qubit couplings ($\tilde{\epsilon} > 1$) the violation of the LGI is small compared with the strong inter-qubit coupling result in the range of $0 < \tilde{\tau} < 1$. However, for $1 < \tilde{\tau} < 5$ that behavior is reversed and the classical non-violation regime prevails ($F(0, \tilde{\tau}, 2\tilde{\tau}) < 1$). Moreover, in the weak inter-qubit coupling the LGI violation stands for longer times. By decreasing the qubit splitting $\tilde{\epsilon}$ the LGI violation is becomes large for short times, as can be seen in Fig.1. For the special case $\tilde{\epsilon} = 1$, the LGI violation breaks down for any $\tilde{\tau}$ and the classical behavior emerges, as should be for a quantum system in contact with an infinite temperature bath as pointed out above.

Now, the essential question is: can the LGI violation be enhanced by a temperature gradient or equivalently by a heat

current? This is analyzed by plotting in Fig. 2 (a) the MLGI as a function of \mathcal{J} and the mean temperature $\tilde{T}_M = (\tilde{T}_1 + \tilde{T}_2)/2$. The variation of MLGI vs. heat current (or equivalently tem-

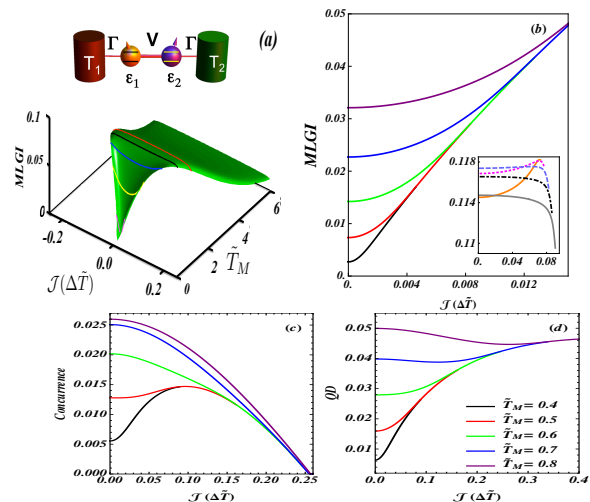


FIG. 2: (Color online). Composite quantum system in contact with two separate thermal reservoirs. (a) A 3D plot of the *first* MLGI (for $\tilde{\tau} = \pi/6$) as a function of mean temperature and heat current for a two-spin chain with $\tilde{\epsilon} = 3$ and $\tilde{\Gamma} = 0.05$ is shown. (b) Slices taken from the 3D left panel are shown for different \tilde{T}_M . Notice that for the lowest values of \tilde{T}_M , MLGI increases with the application of a temperature gradient. Similar results are shown in the inset for higher mean temperatures: Orange ($\tilde{T}_M = 2.25$), magenta ($\tilde{T}_M = 2.5$), purple ($\tilde{T}_M = 2.75$), black ($\tilde{T}_M = 3.0$), gray ($\tilde{T}_M = 3.25$). A qualitatively similar behavior can be observed for the two-spin chain concurrence (c) and quantum discord (d) as a function of the heat current. The color convention for curves in (b-main figure), (c) and (d) is the same. Since the values of $\tilde{\epsilon}$ are the same, a symmetric curve is obtained for $\Delta\tilde{T} < 0$.

perature gradient) changes its concavity indicating that the enhancement of LGI violations under nonequilibrium thermal conditions is restricted to the low mean temperature sector. This behavior can be understood as a competition of the coherent flip-flop spin processes (dominated by the V term) and a temperature dependent decay rate ($\tilde{\Gamma}_V$), as can be deduced from Eq. 7. Since $\tilde{\Gamma}_V \ll 1$, it is possible to obtain an analytical expression for the MLGI as $MLGI \simeq r_{23} \left[e^{-\frac{\pi\tilde{\Gamma}_V}{6}} + \frac{1}{2} e^{-\frac{\pi\tilde{\Gamma}_V}{3}} - 1 \right]$, that depends on the product of the stationary spin chain level populations r_{23} and an effective decay term. For low \tilde{T}_M , and $\Delta\tilde{T} \ll 2\tilde{T}_M$, the population term in the last analytical MLGI expression is much more important than the effective decay indicating that the MLGI starts to grow as the r_{23} increases for $\Delta\tilde{T} = 0$. By contrast, for higher \tilde{T}_M it is very easy to demonstrate that r_{23} decreases faster than the contribution of the effective decay $\tilde{\Gamma}_V$ indicating that the decay term dominates and the flip-flop interaction does not contribute appreciably due to the fact that the population of each eigenstate is saturated at 1/4. This is the main reason why moving away from thermal equilibrium the MLGI decreases for high \tilde{T}_M . The non-equilibrium enhancement of spatial quantum coherences in the same spin-chain system,

as measured by the concurrence [15] and QD [21], is shown in Fig. 2 (c)-(d), respectively. This correspondence between spatial and temporal correlations extends to a nonequilibrium thermal setting previous observations of a perfect mapping between Bell inequality and LGI [30].

Our method as applied to the single spin case [4, 6] (results not shown here) demonstrates that MLGI is not enhanced, rather it is suppressed, when a nonequilibrium temperature gradient is applied. Therefore, a two-qubit system is the smallest spin chain where nonequilibrium enhancement of LGI violations can be observed.

A complete presentation of LGI violations under nonequilibrium conditions is given in Fig.3 (a) We point out that ther-

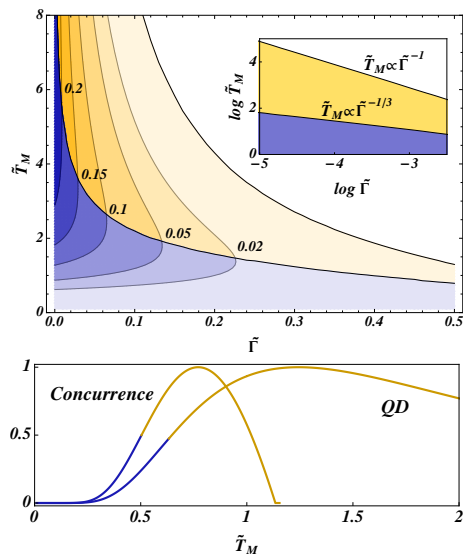


FIG. 3: (Color online). (a) Contour plot of MLGI in the $(\tilde{\Gamma}, \tilde{T}_M)$ parameter space for $\tilde{\epsilon} = 3$. The numbers around the contour lines give the values of the MGLI at $\Delta\tilde{T} = 0$. Inset: $(\tilde{\Gamma}, \tilde{T}_M)$ in log-log scales showing power laws for the borderlines between different non-equilibrium MLGI behavior regions. (b) Typical behaviors of concurrence and QD at equilibrium (both normalized to their maximum value), where a blue line indicates that a temperature gradient increases the quantum spatial correlation while a yellow line indicates that a temperature gradient decreases the quantum spatial correlation.

mal nonequilibrium effects on LGI violations can be grouped in three zones in the whole $(\tilde{\Gamma}, \tilde{T}_M)$ parameter space. First, there are no LGI violations, both in equilibrium and nonequilibrium, for sufficiently high $\tilde{\Gamma}$ or \tilde{T}_M values, corresponding to the upper right white zone in Fig. 3 (a). This behavior is consistent with the deleterious effect of strong coupling or high temperature on quantum correlations. Second, there is a zone with intermediate values of $\tilde{\Gamma}$ and \tilde{T}_M (yellow region in Fig.3 (a) where $MLGI > 0$ at thermal equilibrium, but the MLGI starts deteriorating rather than improving as the system is subject to a small temperature gradient. As shown in the inset, where a log-log scale has been used for $\tilde{\Gamma}$ and \tilde{T}_M , the numerically determined borderline between the white and yellow zones has a power law expression such that $\tilde{T}_M \sim \tilde{\Gamma}^{-1}$.

This simple relation can be easily justified by using our analytical approximation for MLGI, by searching for the $(\tilde{\Gamma}, \tilde{T}_M)$ values yielding to a null value for MLGI at $\Delta\tilde{T} = 0$. Third, and most importantly, there is a parameter region of low $\tilde{\Gamma}$ or \tilde{T}_M values (blue zone in Fig.3 (a) where the equilibrium value of MLGI is further increased as the system is taken out of equilibrium by setting a temperature gradient. The numerically determined borderline between the yellow and blue regions in Fig.3 (a) satisfies also a power law of the form $\tilde{T}_M \sim \tilde{\Gamma}^{-1/3}$. This behavior can also be explained by requiring that $\frac{\partial^2 MLGI}{\partial(\Delta\tilde{T})^2}|_{\Delta\tilde{T}=0} = 0$, to obtain[29]

$$\tilde{\Gamma} = \frac{3}{\pi} \left[\frac{\tilde{\epsilon}}{4} \right]^3 \left[1 - \left(\frac{1}{\tilde{\epsilon}} \right)^4 \right] \frac{1}{\tilde{T}_M^3} \quad (8)$$

in agreement with the numerical results plotted in Fig. 3 (a). Clearly, when $V \geq \epsilon$ no solution for Eq.(8) exists indicating that a requirement for the thermal nonequilibrium enhancement of LGI violations is that spins are in the weak coupling regime. By contrast with two-time quantum correlations, two-point spatial correlations in the steady-state do not depend on the quantum system coupling strength with the thermal baths. However, as shown in Fig.3 (b), the two-spin concurrence and QD also present a nonequilibrium thermal enhancement at low enough temperatures signaling one more time the correspondence between temporal and spatial quantum correlation behaviors. As it has already been documented the QD persists up to larger temperatures as compared with the concurrence.

In summary, we have provided a microscopic derivation of LGI, for a spin chain coupled to two reservoirs at different temperatures. Nonequilibrium thermal quantum correlations have been analyzed exactly by mapping the original two-*interacting* spins coupled chain to an equivalent system of two-noninteracting spins, each one of them in contact with a renormalized heat reservoir at an effective temperature. Based on a Kraus-operator approach, we demonstrate that in a certain range of temperature gradients the steady-state LGI violation can be enhanced. The frontiers between different behaviors of the MLGI response to thermal nonequilibrium conditions have been found to be characterized by power laws relating mean temperature of the heat reservoirs and the spin chain coupling strength with the baths. This leads to the interesting feature that nonequilibrium thermal conditions provide the opportunity to enhance not only spatial but also temporal quantum correlations.

We acknowledge Susana Huelga and Neil F. Johnson's critical readings of the manuscript and Facultad de Ciencias, Vicerrectoría de investigaciones at Universidad de los Andes, for financial support to the project *Quantum control of Non-Equilibrium hybrid systems* (2012-2014).

[1] J. S. Bell, Physics **1**, 195 (1964).

[2] A. J. Leggett and A. Garg, Phys. Rev. Lett. **54**, 857 (1985).

- [3] J. P. Paz and G. Mahler, Phys. Rev. Lett. **71**, 3235 (1993).
- [4] S. F. Huelga, T. W. Marshall and E. Santos, Phys. Rev. **A54**, 1798 (1996).
- [5] J. Kofler and C. Brukner, Phys. Rev. Lett. **101**, 090403 (2008).
- [6] N. Lambert, R. Johansson and F. Nori, Phys. Rev. **B84**, 245421 (2011).
- [7] A. Palacios-Laloy, F. Mallet, F. Nguyen, P. Bertet, D. Vion, D. Esteve and A. N. Korotkov, Nature Phys. **6**, 442 (2010).
- [8] M. E. Goggin, M. P. Almeida, M. Barbieri, B. P. Lanyon, J. L. O'Brien, A. G. White and G. J. Pryde, Proc. Acad. Nat. Sci. **108**, 1256 (2011).
- [9] G. C. Knee, S. Simmons, E. M. Gauger, J. J.L. Morton, H. Riemann, N. V. Abrosimov, P. Becker, H.-J. Pohl, K. M. Itoh, M. L.W. Thewalt, G. A. D. Briggs and S. C. Benjamin, Nat. Commun. **3**:606 doi:10.1038/ncomms1614 (2012).
- [10] A. N. Jordan, A. N. Korotkov and M. Büttiker, Phys. Rev. Lett. **97**, 026805 (2006)
- [11] V. Athalye, S. Singha Roy and T. S. Mahesh, Phys. Rev. Lett. **107**, 130402 (2008).
- [12] G. Waldherr, P. Neumann, S. F. Huelga, F. Jelezko and J. Wrachtrup, Phys. Rev. Lett. **107**, 090401 (2011).
- [13] J.-S. Xu, C.-F. Li, X.-B. Zou and G.-C. Guo, Sci. Rep. **1**, 101; doi:10.1038/srep00101 (2011); J.-S. Xu, C.-F. Li, C.-J. Zhang, X.-Y. Xu, Y.-S. Zhang and G.-C. Guo, Phys. Rev. **A82**, 042328 (2010).
- [14] J. Dressel, C. J. Broadbent, J. C. Howell and A. N. Jordan, Phys. Rev. Lett. **106**, 040402 (2011).
- [15] L. Quiroga, F. J. Rodríguez, M. E. Ramírez and R. París, Phys. Rev. **A75**, 032308 (2007).
- [16] A. Polkovnikov, K. Sengupta, A. Silva and M. Vengalattore, Rev. Mod. Phys. **83**, 863 (2011).
- [17] M. A. Cazalilla, A. Iucci and M.-C. Chung, Phys. Rev. **E85**, 011133 (2012).
- [18] M.B. Plenio and S. Huelga, Phys. Rev. Lett. **88**, 197901 (2002).
- [19] I. Sinayski, F. Petruccione and D. Burgarth, Phys. Rev. **A78**, 062301 (2008).
- [20] N. Lambert, R. Aguado and T. Brandes, Phys. Rev. **B75**, 045340 (2007).
- [21] L.-A. Wu and D. Segal, Phys. Rev. **A84**, 012319 (2011).
- [22] M. Greiner, O. Mandel, T. Hansch and I. Bloch, Nature **419**, 51 (2002).
- [23] R.W. Simmonds, K.M. Lang, D. A. Hite, S. Nam, D. P. Pappas and John M. Martinis, Phys. Rev. Lett. **93**, 077003 (2004).
- [24] M. Sarovar, A. Ishizaki, G. R. Fleming and K. B. Whaley, Nat. Phys. **6**, 462 (2010).
- [25] M. Scully, Phys. Rev. Lett. **87**, 220601 (2001).
- [26] F. Giazotto, and M. Martínez Pérez, Nature **492**, 401 (2012).
- [27] D. Avis, P. Hayden, and M. M. Wilde, Phys. Rev. **A82**, 030102(R) (2010).
- [28] K. Kraus, *States, Effects and Operations: Fundamental Notions of Quantum Theory*. (Springer Verlag, 1983).
- [29] See Supplementary Information.
- [30] S. Marcovitch and B. Reznik, quant-ph/1107.2186.